JOURNAL OF PROPULSION AND POWER
Vol. 27, No. 2, March–April 2011

Technical Notes

Control-Oriented Model for Intake Shock Position Dynamics in Ramjet Engine

Ik-Soo Park*
Korea Advanced Institute of Science and Technology, Daejeon 305-701, Republic of Korea
Sun-Kyoung Kim,† Hyo-Won Yeom,‡ and Hong-Gye Sung§
Korea Aerospace University, Goyang, Gyeonggido 412-791, Republic of Korea
and
Jung-Woo Park¶ and Min-Jea Tahk**
Korea Advanced Institute of Science and Technology, Daejeon 305-701, Republic of Korea

DOI: 10.2514/1.B34008

I. Introduction

RAMJET-POWERED engines have a history of over 100 years [1]. The secret to efficiency, safety, and performance of ramjet combustion systems has been the correct location and control of the terminal shock in the intake duct [2]. The position of the intake shock is affected by perturbations propagating upstream from the combustor [3] and from disturbances in the freestream [4]. These can lead to the familiar instability problems of unstart or buzz [5,6]. At the same time, these very instabilities can be controlled by pressure perturbations injected by suitably manipulating the exhaust nozzle throat area [7]. To properly evaluate such a control, it is necessary to obtain a model for the ramjet engine including the intake, combustor, and exhaust nozzle.

The issue of shock position control has always been an interesting one [8], but accurately sensing the position of the intake shock for the purpose of active control has been a challenge. In recent years, though, the problem has attracted much attention [9,10], and building on the earlier work on the dynamics of shocks in ducts [3,11], models that may be used for designing intake shock position controllers have been obtained [12,13]. However, it may be noted that all these models were limited to the intake alone and hence could not be directly used to study the effect of the exhaust nozzle throat area variation on the intake shock location.

A model that couples the intake with the combustor and exhaust nozzle for a ramjet was first realized recently by our coworkers [14], and it was used [15] to derive a control law for the intake shock location using the nozzle throat area as input. A significant feature of the model in [14] was the use of time lags to capture the physics of upstream and downstream propagating waves between the intake and combustor. However, these time lags were applied to the primitive variables for simplicity instead of the specific pressure or entropy waves [12]. Second, despite the relatively low order of the global model in [14], the model for each component was multiparameter and nonlinear, in order to capture the various physical phenomena in the intake and combustor. Thus, in deriving the control law in [15], local linearized reduced-order models at several operating points had to be obtained using a system identification tool. The system identification is, unfortunately, a mathematical procedure that results in a set of states that cannot be easily related to the physical variables, thus masking the physical relationships inherent in the system. Control of the terminal shock position was obtained indirectly in [15] by defining a related parameter called intake backpressure margin.

The present Note differs from these previous works in three significant ways. First, we write an explicit equation for the dynamics of the intake shock location in a coupled model of the intake and the combustor plus nozzle. Second, a single time-lag parameter is obtained numerically, and applied directly to the shock position variable. Third, the various component models are written using standard quasi-one-dimensional flow relations in such a manner that the physical relationships they represent are apparent. These features make the present model more suitable for controller design with the objective of regulating the intake shock position; hence, it is called a control-oriented model.

II. Terminal Shock Equilibrium Model

A typical ramjet engine consists of four parts, supersonic intake, subsonic diffuser, combustor, and supersonic nozzle, as shown in Fig. 1. Depending on the distinguishing flow properties, the parts are subdivided into nine internal sections by the node points numbered as in Fig. 1. Variables at each node are labeled as T_7, and so on, and the total (stagnation) value by T_{07}, etc.

A. Supersonic Compression

Supersonic flow is compressed externally between nodes 0 and 1 by one or more oblique shocks and internally between nodes 1 and 2 by a series of weak shocks until the terminal shock at node 2. For supercritical flow, node 1 properties are the same as the freestream; hence, the given freestream flow properties and angle of attack, the total temperature T_{01}, total pressure P_{01}, and intake air mass flow rate $\dot{m}_1$ at node 1 can be determined from the assumption of calorically perfect gas, adiabatic process, oblique shock relation, and predetermined air-capture ratio as a function of angle of attack and flight Mach number.

The mass flow rate and total temperature at node 2 are the same as those at node 1 from mass conservation and assumption of adiabatic process, but the total pressure is different. The pressure-loss coefficient η_{02} between the freestream and node 2 is obtained numerically as in [14,16] and recorded in tabular form as a function of freestream Mach number M and angle of attack as

$$\eta_{02} = f(M_1, \alpha) \tag{1}$$

Note that node 2 is not fixed to the body, but moves with the terminal shock. Hence, an average position of the shock is used to define the domain for the numerical analysis.

Received 9 May 2010; revision received 17 November 2010; accepted for publication 24 November 2010.

*Ph.D. Student, School of Mechanical, Aerospace and System Engineering; ispak@fdcl.kaist.ac.kr.

†M.A. Student, School of Aerospace and Mechanical Engineering; soaring7@kau.ac.kr.

‡Ph.D. Student, School of Aerospace and Mechanical Engineering; hwyeum@kau.ac.kr.

§Professor, School of Aerospace and Mechanical Engineering; hgsung@kau.ac.kr. Associate Fellow AIAA.

¶Ph.D. Student, School of Mechanical, Aerospace and System Engineering; jwpark@fdcl.kaist.ac.kr.

**Professor, School of Mechanical, Aerospace and System Engineering; mjtahk@fdcl.kaist.ac.kr. Member AIAA.

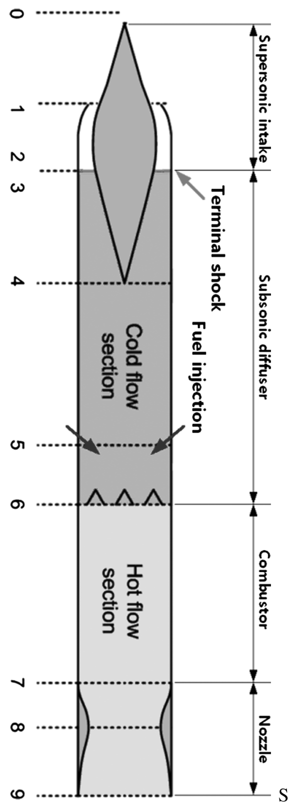

Fig. 1 Section view and node definition of typical ramjet engine.

B. Subsonic Diffusion and Combustion

The subsonic segment flow properties must be determined starting from the nozzle and then progressing upstream. The flow properties at node 7 can be obtained by assuming the nozzle to be choked. The Mach number M_7 and mass flow rate $\dot{m}_7$ are determined from the Mach number area relation for the nozzle and mass conservation, respectively. The total temperature T_{07} is obtained by use of the CEA (Chemical Equilibrium with Applications) code and made into a tabular form as a function of equivalence ratio (EQ) and total temperature T_{06}. The total pressure P_{06} may be obtained by using the Rayleigh flow relation between nodes 6 and 7 [17]. The total temperature T_{06} and mass flow rate $\dot{m}_6$ at node 6 can be obtained from upstream conditions by assuming adiabatic process and mass conservation. Finally, the flow between nodes 3 and 6 can be modeled as Fanno flow, so the total pressure P_{03} can be determined from the Fanno relation [17].

C. Matching Condition

The properties at node 2 from the upstream supersonic flow and those at node 3 from the downstream subsonic flow, on either side of the terminal shock, are matched by using the normal shock relations [17]. A schematic is shown in Fig. 2. For a stationary shock, the equilibrium state of the diffuser internal flow follows the Mach number area relation. Therefore, the area A_{ss}, at which the terminal shock is located in the steady state, can be obtained from the mass conservation and isentropic relations as follows:

$$A_{ss} = \frac{\dot{m}_2}{P_{02}\sqrt{\frac{\gamma}{RT_{02}}\left(\frac{2}{\gamma+1}\right)^{\frac{\gamma+1}{\gamma-1}}}}\frac{1}{M_2}\left[\left(\frac{2}{\gamma+1}\right)\left(1+\frac{\gamma-1}{2}M_2^2\right)\right]^{\frac{\gamma+1}{2(\gamma-1)}} \tag{2}$$

where $\dot{m}_2$, P_{02}, T_{02}, and γ are, respectively, mass flow rate, total pressure, total temperature, and specific heat ratio at node 2. The Mach number M_2 can be determined from the normal shock relation as a function of total pressure ratio between nodes 2 and 3, as below:

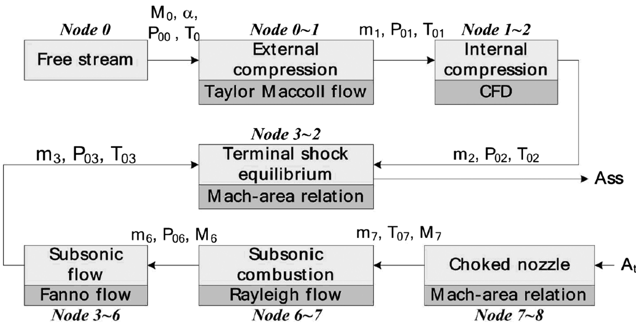

Fig. 2 Determination procedure of steady variables of internal flow.

$$\frac{P_{03}}{P_{02}} = \left[\frac{\frac{\gamma+1}{2}M_2^2}{1+\frac{\gamma-1}{2}M_2^2}\right]^{\frac{\gamma}{\gamma-1}}\left[\frac{1}{\frac{2}{\gamma+1}M_2^2+\frac{\gamma-1}{\gamma+1}}\right]^{\frac{1}{\gamma-1}} \tag{3}$$

Any effects on the intake flow properties due to shock motion in the intake duct are neglected. Thus, for example, the shock position determined above does not consider the change of total pressure P_{02} in a moving frame attached to the moving shock. In general, the variation in P_{02} due to the shock motion is small compared with the subsonic total pressure P_{03}, provided the extent of shock travel is limited. Simulation results also bear out this assumption when applied to supersonic intakes having a weak terminal shock, which is the case for most ramjets.

III. Terminal Shock Dynamic Model

A change in the nozzle throat area takes a small but finite time to influence the combustor pressure, as modeled by the B parameter in [14,15]. Then the upstream propagating pressure wave from the combustor affects the intake shock position, which then generates a new total pressure at node 3 behind the terminal shock. This revised total pressure is conveyed downstream where it alters the combustor flow properties. Finally, an updated equilibrium condition can be obtained after several sweeps of the upstream pressure wave and downstream entropy and pressure waves. In previous work [14], each of these propagation phenomena were individually represented by appropriate time lags, which meant that all the intermediate variables at stations 4–7 had to be dynamic in nature. Instead, in this work, we prefer to write only a single dynamic equation for the intake shock position. Hence, we desire a single time-lag parameter that is an aggregate of all the various time lags between the various stations considered in [14]. This is obtained by an unsteady numerical simulation, as in [16], by introducing a perturbation in combustor pressure, recording the change in the intake shock location, and fitting a first-order response to get an estimate of the time constant. The resulting dynamic equation for the intake shock position is

$$\tau\dot{A}_s = -A_s + A_{ss} \tag{4}$$

where τ is the time constant, and A_s is the instantaneous position of the shock given by the corresponding intake duct area. The steady-state shock location A_{ss} is a function of the fuel flow rate and nozzle throat area.

The time lag between application of nozzle throat area control input and change in combustor pressure is accommodated in the nozzle actuation dynamics. Similarly, there is a time lag associated with liquid-fuel injection, mixing, evaporation, and gaseous fuel burn, leading to an increase in combustor total temperature and pressure. This delay is factored into the fuel supply system dynamics. Thus, the time constant τ in Eq. (4) represents only the time delay from combustor pressure change to terminal shock location.

Equation (4) shows stable dynamical behavior; stability of the shock dynamics is not an issue as only the supercritical intake case is considered.

Table 1 Comparison of shock position for different simulation conditions

Simulation condition		Input parameters		Area at shock position, m^2	
Mach no.	Altitude, km	EQ	NA	Higher-fidelity model [18]	Present model
2.1	1.0	1.0	0.54	0.0097	0.0098
2.1	1.0	1.0	0.64	0.0122	0.0123
2.1	1.0	0.6	0.54	0.0129	0.0128
2.1	1.0	0.6	0.64	0.0153	0.0153
3.0	15.0	1.0	0.54	0.0132	0.0132
3.0	15.0	1.0	0.64	0.0155	0.0157
3.0	15.0	0.6	0.54	0.0157	0.0157
3.0	15.0	0.6	0.64	0.0181	0.0186

IV. Simulation Results

Simulations are reported for two flight conditions: Mach 2.1 with 1.0 km altitude and Mach 3.0 with 15.0 km altitude. For each case, combinations of two values for each input parameter are considered, as listed in Table 1: EQ of 1.0 and 0.6 and nozzle throat area normalized by the maximum value, NA, of 0.54 and 0.64. The equilibrium shock location predicted by the present model (model for controller design) is seen to compare very well with that from a higher-fidelity model (integral performance model) proposed by Kim et al. [18]. That model has been constructed with physical gas and thermodynamic models (satisfying mass, momentum, and energy conservation) through an entire flowpath for major parts: supersonic air intake performance model, combustor analysis model, and dynamic model of the fuel supply system. The supersonic air intake model performs shock train analysis based on the Oswatitsch criterion. The loss effects in the engine are considered by defining the efficiency coefficients of each component with flow variables, which is verified with numerical and experimental data. Quasi-one-dimensional combustor analysis with variable thermodynamic properties determined from CEA embedded in the analysis model is implemented to observe detailed characteristics of the internal flow properties in the combustor. The dynamic models of the fuel supply system and interaction between combustor pressure fluctuation and terminal shock train are considered to determine their mutual relations and operating margin.

The internal steady-state flow variables, Mach number, static pressure, and static temperature at various stations (nodes 0, 4, 6, 7, and 9 in Fig. 1) for the two flow conditions are shown in Figs. 3 and 4. Each figure has subfigures for different combinations of the parameters EQ and NA. From the freestream to the combustor inlet, the Mach number decreases, in contrast to the static pressures and temperatures in terms of supersonic compression and subsonic deceleration. As the subsonic combustion takes place in the combustor, Mach number and static temperature increase (for specified incoming flow Mach number), whereas the static pressure decreases as the subsonic Rayleigh flow decreases. Both the static pressure and temperature increase as increasing of EQ in fuel-lean region. Obviously, Mach number and static pressure have opposite tendency as increasing NA. For the different Mach number and flight altitude conditions, only the Mach number is decelerated rapidly in supersonic region of intake, and the other variables move in a similar manner, with only magnitude differences. It can be seen that the present model accurately predicts the flow variables at internal stations in all cases and shows a good match with the higher-fidelity model in [18].

Finally, Fig. 5 shows the dynamic response of the intake shock to a sequence of step changes in the nozzle throat area for the Mach 3.0, 15.0 km altitude case, with EQ held fixed at 1.0. As the nozzle throat is decreased from NA of 0.64 as a starting point of simulation to NA of 0.54, the terminal shock moves upward to its inlet cowl lip, but downward as increasing nozzle throat area showing the same steady-state value in Table 1. From the dynamics point of view, the first-order response is clearly visible and the settling time can be estimated to be 0.297 s, as expected from the time constant of Eq. (4).

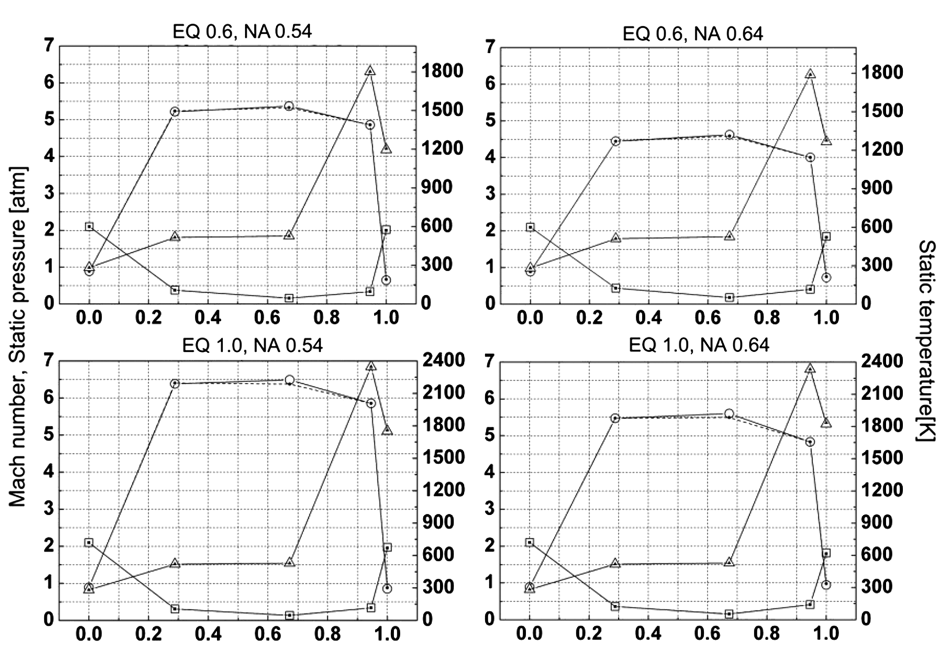

Fig. 3 Internal flow variables for Mach 2.1, 1.0 km altitude for different EQ and NA from model for performance analysis (open symbols) and model for controller design (filled symbols): Mach number (rectangle), static pressure (circle), and static temperature (triangle).

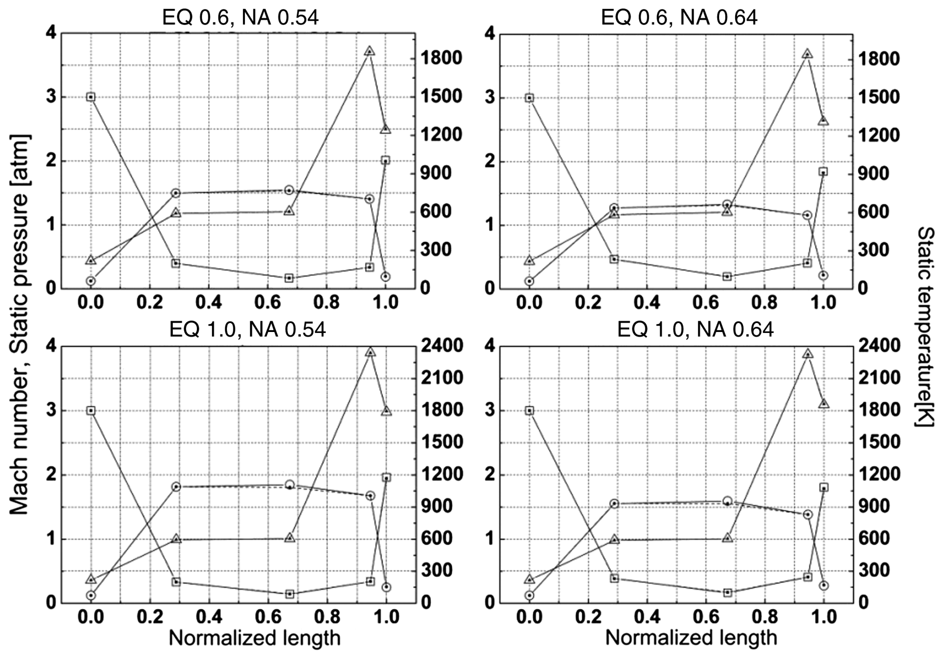

Fig. 4 Internal flow variables for Mach 3.0, 15.0 km altitude for different EQ and NA from model for performance analysis (open symbols) and model for controller design (filled symbols): Mach number (rectangle), static pressure (circle), and static temperature (triangle).

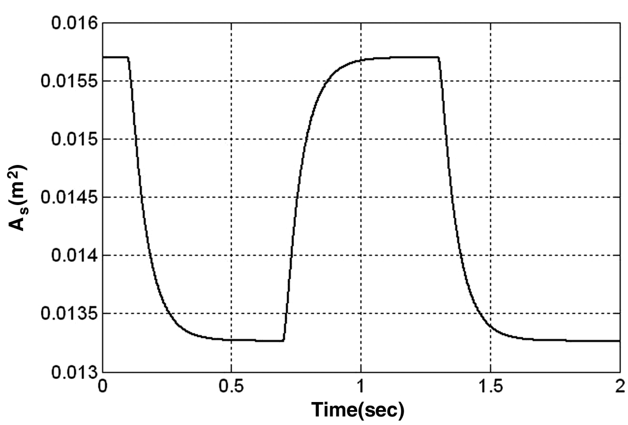

Fig. 5 Response of shock position to a sequence of step changes of nozzle throat area for Mach 3.0, altitude 15.0 km and EQ 1.0; *y* axis is intake duct area at the location of terminal shock, A_s.

V. Conclusions

The present work has described a simple, yet highly accurate, first-order dynamical model for the dynamics of the terminal shock in the intake duct of a ramjet engine. Unlike previous work on intake shock position control, the model accounts for the coupling between the intake and the combustor plus exhaust nozzle. Equilibrium flow models for the supersonic intake and the subsonic diffuser and combustor are matched at the terminal shock location in the duct. The total pressures across the shock can then be related to the upstream Mach number and hence to the area of the duct where the shock is located. A first-order dynamical model for the shock position is written in terms of the corresponding duct area as the state variable. By using a single aggregate time lag obtained directly from an unsteady numerical flow simulation, it is not necessary to consider other internal flow variables as states of the dynamical system. The present model is therefore suitable for design of shock position controllers for ramjet engines.

References

[1] Fry, R. S., "A Century of Ramjet Propulsion Technology Evolution," *Journal of Propulsion and Power*, Vol. 20, No. 1, Jan.–Feb. 2004, pp. 27–58.
doi:10.2514/1.9178

[2] Himmel, S. C., "Some control considerations for ram-jet engines," NACA RM-E52F10, 1952.

[3] Hurrell, H. G., "Analysis of Shock Motion in Ducts during Disturbances in Downstream Pressure," NASA TN-4090, 1957.

[4] Mayer, D. W., and Paynter, G. C., "Prediction of Supersonic Inlet Unstart Caused by Freestream Disturbances," *AIAA Journal*, Vol. 33, No. 2, 1995, pp. 266–275.
doi:10.2514/3.12418

[5] Sterbentz, W., and Evvard, J., "Criterions for Prediction and Control of Ram-Jet Flow Pulsations," NACA RM E51C27, 1951.

[6] Trimpi, R., "A Theory for Stability and Buzz Pulsation Amplitude in Ram Jets and an Experimental Investigation Including Scale Effects," NACA Rept. 1265, 1956.

[7] Boksenbaum, A. S., and Novik, D., "Control Requirements and Control Parameters for a Ram Jet with Variable-Area Exhaust Nozzle," NACA RM E8H24, Nov. 1948.

[8] Vasu, G., Wilcox, F. A., and Himmel, S. C., "Preliminary Report of Experimental Investigation of Ram-jet Controls and Engine Dynamics," NACA RM-E54H10, 1954.

[9] Ohshima, T., Kanbe, K., Kimura, H., Fujiwara, K., Suzuki, K., and Yanagi, R., "Control of the Intake Shock Position in the Test Rig for Ramjet Engine," AIAA/ASME/SAE/ASEE 33rd Joint Propulsion Conference and Exhibit, AIAA Paper 1997-2885, Seattle, WA, July 1997.

[10] Kopasakis, G., and Connolly, J. W., "Shock Positioning Controls Design for a Supersonic Inlet," AIAA/ASME/SAE/ASEE 45th Joint Propulsion Conference and Exhibit, AIAA Paper 2009-5117, Denver, CO, Aug. 2009.

[11] Culick, F. E. C., and Rogers, T., "The Response of Normal Shocks in Diffusers," *AIAA Journal*, Vol. 21, No. 10, 1983, pp. 1382–1390.
doi:10.2514/3.60147

[12] MacMartin, D., "Dynamics and Control of Shock Motion in a Near-Isentropic Inlet," *Journal of Aircraft*, Vol. 41, No. 4, Jul.–Aug. 2004, pp. 846–853.
doi:10.2514/1.416

[13] Daren, Y., Tao, C., and Wen, B., "Equilibrium Manifold Linearization Model for Normal Shock Position Control Systems," *Journal of Aircraft*, Vol. 42, No. 5, Sept.–Oct. 2005, pp. 1344–1347.
doi:10.2514/1.12845

[14] Gupta, N. K., Gupta, B. K., Ananthkrishnan, N., Shevare, G. R., Park, I. S., and Yoon, H. G., "Integrated Modeling and Simulation of an Airbreathing Combustion System Dynamics," AIAA Modeling and Simulation Technologies Conference and Exhibit, AIAA Paper 2007-6374, Hilton Head, SC, Aug. 2007.

[15] Bharani Chandra, K. P., Gupta, N. K., Ananthkrishnan, N., Park, I. S.,

and Yoon, H. G., "Modeling, Simulation, and Controller Design for an Airbreathing Combustion System," *Journal of Propulsion and Power*, Vol. 26, No. 3, 2010, pp. 562–574.
doi:10.2514/1.42368

[16] Yeom, H.-W., Kim, S.-J., Sung, H.-G., and Yang, V., "Inlet Buzz and Combustion Oscillation in an Axisymmetric Ramjet Engine," 48th AIAA Aerospace Sciences Meeting, AIAA Paper 2010-756, Orlando, FL, 4–7 Jan. 2010.

[17] Farokhi, S., *Aircraft Propulsion*, Wiley, New York, 2009, pp. 17–96.

[18] Kim, S. K., Yeom, H. W., Jeon, J. S., and Sung, H. G., "An Integrated Dynamic Model to Control Ramjet Propulsion System," Proceedings of the KSAS-JSASS Joint International Symposium on Aerospace Engineering, 2008, pp. 467–470.

R. Bowersox
Associate Editor